Contents lists available at ScienceDirect

Urban Forestry & Urban Greening

journal homepage: www.elsevier.com/locate/ufug

Tree effects on urban microclimate: Diurnal, seasonal, and climatic temperature differences explained by separating radiation, evapotranspiration, and roughness effects

Naika Meili [a,b,*], Gabriele Manoli [c], Paolo Burlando [b], Jan Carmeliet [d], Winston T.L. Chow [e], Andrew M. Coutts [f,g], Matthias Roth [h], Erik Velasco [i], Enrique R. Vivoni [j,k], Simone Fatichi [b,l]

[a] Future Cities Laboratory, Singapore-ETH Centre, Singapore
[b] Institute of Environmental Engineering, ETH Zurich, Switzerland
[c] Department of Civil, Environmental and Geomatic Engineering, University College London, UK
[d] Chair of Building Physics, ETH Zurich, Switzerland
[e] School of Social Sciences, Singapore Management University, Singapore
[f] School of Earth, Atmosphere and Environment, Monash University, Clayton, Australia
[g] Cooperative Research Centre for Water Sensitive Cities, Melbourne, Australia
[h] Department of Geography, National University of Singapore, Singapore
[i] Centre for Urban Greenery and Ecology, National Parks Board, Singapore
[j] School of Sustainable Engineering and the Built Environment, Arizona State University, Tempe, Arizona, USA
[k] School of Earth and Space Exploration, Arizona State University, Tempe, Arizona, USA
[l] Department of Civil and Environmental Engineering, National University of Singapore, Singapore

ARTICLE INFO

ABSTRACT

Increasing urban tree cover is an often proposed mitigation strategy against urban heat as trees are expected to cool cities through evapotranspiration and shade provision. However, trees also modify wind flow and urban aerodynamic roughness, which can potentially limit heat dissipation. Existing studies show a varying cooling potential of urban trees in different climates and times of the day. These differences are so far not systematically explained as partitioning the individual tree effects is challenging and impossible through observations alone. Here, we conduct numerical experiments removing and adding radiation, evapotranspiration, and aerodynamic roughness effects caused by urban trees using a mechanistic urban ecohydrological model. Simulations are presented for four cities in different climates (Phoenix, Singapore, Melbourne, Zurich) considering the seasonal and diurnal cycles of air and surface temperatures.

Results show that evapotranspiration of well-watered trees alone can decrease local 2 m air temperature at maximum by 3.1– 5.8 °C in the four climates during summer. Further cooling is prevented by stomatal closure at peak temperatures as high vapour pressure deficits limit transpiration. While shading reduces surface temperatures, the interaction of a non-transpiring tree with radiation can increase 2 m air temperature by up to 1.6 – 2.1 °C in certain hours of the day at local scale, thus partially counteracting the evapotranspirative cooling effect. Furthermore, in the analysed scenarios, which do not account for tree wind blockage effects, trees lead to a decrease in urban roughness, which inhibits turbulent energy exchange and increases air temperature during daytime. At night, single tree effects are variable likely due to differences in atmospheric stability within the urban canyon. These results explain reported diurnal, seasonal and climatic differences in the cooling effects of urban trees, and can guide future field campaigns, planning strategies, and species selection aimed at improving local microclimate using urban greenery.

* Corresponding author at: Future Cities Laboratory, Singapore-ETH Centre, Singapore.
E-mail addresses: meili@ifu.baug.ethz.ch (N. Meili), g.manoli@ucl.ac.uk (G. Manoli), paolo.burlando@ifu.baug.ethz.ch (P. Burlando), cajan@ethz.ch (J. Carmeliet), winstonchow@smu.edu.sg (W.T.L. Chow), Andrew.Coutts@monash.edu (A.M. Coutts), geomr@nus.edu.sg (M. Roth), evelasco@mce2.org (E. Velasco), vivoni@asu.edu (E.R. Vivoni), ceesimo@nus.edu.sg (S. Fatichi).

1. Introduction

The increase of vegetation in cities is often promoted by urban planners and policy-makers to increase liveability and solve environmental challenges imposed by urbanization (Pataki et al., 2011). Urban greenery provides multiple ecosystem services, such as climate regulation (Bowler et al., 2010; Konarska et al., 2016; Manoli et al., 2019), storm water retention (Berland et al., 2017), improved biodiversity (Grimm et al., 2008), and cultural, aesthetic, and health benefits (Salmond et al., 2016; Willis and Petrokofsky, 2017; Ng et al., 2018). Urban vegetation consisting of lawns, shrubs, trees, forests, and green roofs and facades all provide unique ecosystem services (Tan et al., 2014; Ossola et al., 2016; Mexia et al., 2018; Fung and Jim, 2019; Richards et al., 2020) but in particular, the increase in urban tree cover is encouraged to improve the outdoor thermal comfort of city dwellers (Shashua-Bar et al., 2011; Morakinyo et al., 2017), as well as decrease building energy consumption for indoor cooling (Wang et al., 2016).

Many measurement as well as modelling studies analyse the effects of tree cover on urban air temperature, however with mixed results (Table 1). Daytime air temperature cooling with varying magnitude is reported by a number of authors. For example, Ziter et al. (2019) find an air temperature decrease of 0.7 °C – 1.5 °C for a maximum tree cover increase in Madison, Wisconsin at a radius of 10 to 90 m, while Konarska et al. (2016) measure an average daytime air temperature reduction of 0.5 °C – 1 °C due to trees within street canyons in Gothenburg, and Shashua-Bar et al. (2009) report air temperature cooling of up to 1.7 °C within a back lane with trees in the Negev Highlands, Israel. Similarly, model simulations by Middel et al. (2015) show a rather large air temperature decrease of 2 °C for a tree canopy increase from 10 % to 15 % in Phoenix, Arizona. In contrast, Coutts et al. (2016) measured only a marginal air temperature reduction at high tree cover at street canyon level in Melbourne, and Armson et al. (2013) find no significant air temperature differences in the sun or shade of street trees in the city of Manchester, UK. Interestingly, Shashua-Bar et al. (2009) even measured a daytime air temperature increase due to a shading mesh over a street canyon in the Negev Highlands, which could be attributed to the radiation and aerodynamic effects of non-transpiring street tree-like structures. Authors analysing the night time air temperature effects of urban trees also report diverging findings, with observed night time warming

Table 1
Examples of contrasting tree effects on urban air temperature during day- and night reported by studies based on field observations in different cities.

City	Spatial scale	$\Delta T_{air,day}$ (°C)	$\Delta T_{air, night}$ (°C)	Reference
Madison, Wisconsin	Radius 10 / 30 / 60 or 90 m	−0.7 / -1.3 / <-1.5	−0.3 to -0.5	(Ziter et al., 2019)
Beijing city	Woodland patch	−0.7 to -5.7		(Jiao et al., 2017)
Gothenburg	Street canyon	−0.5 to -1	+0.2 to +0.6	(Konarska et al., 2016)
Negev Highlands	Street canyon	−1.7	> 0	(Shashua-Bar et al., 2009)
Melbourne	Street canyon	0*		(Coutts et al., 2016)
Dresden	Within tree canopy	−0.8 to -2.2		(Gillner et al., 2015)
Munich	Within tree canopy	−0.9 to -1.6	−0.3 to -0.4	(Rahman et al., 2019)
Munich	Within tree canopy	max -3.5	+0.5	(Rahman et al., 2017)
Munich	Within tree shade	−0.7 to -0.8		(Rahman et al., 2017)
Manchester	Within tree shade	0*		(Armson et al., 2013)
Negev Highlands	Shade mesh in street canyon	1		(Shashua-Bar et al., 2009)

* no significant effects.

(Shashua-Bar et al., 2009; Konarska et al., 2016; Rahman et al., 2017) as well as cooling (Rahman et al., 2019; Ziter et al., 2019).

The contrasting effects of urban trees on air temperature are likely caused by differences in methodological approaches, spatial (tree vs. neighbourhood vs. city scale) and temporal scales (hourly vs. daily vs. seasonal) of observation, modelling assumptions, and baseline climate, but so far there is no clear explanation for such discrepancies. Furthermore, changes in air temperature due to tree cover are not uniform throughout the day but vary on sub-daily timescales with a stronger temperature decrease observed and simulated during morning or afternoon hours than during midday (Shashua-Bar et al., 2009; Morakinyo and Lam, 2016; Salmond et al., 2016). Understanding the diurnal cycle of air temperature change caused by trees is important to accurately assess their cooling potential during the hottest hours of the day or at times when it is most needed, e.g., because of prevalent outdoor activities.

Studies explaining the mechanisms through which urban trees modify the diurnal evolution of air temperature are fragmented. Trees alter the urban climate due to several effects, such as their interaction with radiation, which leads to shading and cooling of surfaces (e.g., Armson et al., 2013; Middel et al., 2016; Upreti et al., 2017). Tree evapotranspiration uses part of the absorbed radiation energy resulting in evapotranspirative cooling effects (Konarska et al., 2015, 2016; Rahman et al., 2018), which might be limited though by environmental factors, such as water availability. Furthermore, the tree structure blocks wind flow due to drag effects (Manickathan et al., 2018; Zölch et al., 2019) and alters the aerodynamic roughness of the urban fabric (Giometto et al., 2017; Kent et al., 2017). Assessment of only one of the aforementioned tree effects on urban climate, such as shade provision by trees, is common in simulation studies (e.g., Wang et al., 2016; Upreti et al., 2017; Wang et al., 2018) because of the complexity of resolving all tree-urban climate interactions at large spatial scales. On the other hand, observational studies that partition the different effects of trees on local climate are scarce, since it is experimentally challenging or even impossible to remove one of these effects without affecting the others. On a single tree level, Tan et al. (2018) measured the relative contribution of tree shading and transpiration to air temperature decrease using a set of potted trees subject to different water withholding treatments. However, measurements by Tan et al. (2018) were in close proximity of single trees and are difficult to extrapolate to integrated urban canyon air temperature.

In this study, we describe the diurnal patterns of canopy layer air and surface temperature changes caused by trees at the street canyon level, with the aim of disentangling the different tree effects on urban microclimate, and explain the discrepancies reported in the literature for varying climates and times of the day. To achieve this, we partition the radiation, evapotranspiration, and roughness effects of urban trees, and quantify their individual and combined impacts on the 2 m and above tree canopy air temperature, as well as urban surface temperatures by means of numerical experiments run with the recently developed urban ecohydrological model, Urban Tethys-Chloris (UT&C) (Meili et al., 2020a) in four cities characterized by distinct climates (Phoenix, USA, Singapore, Singapore, Melbourne, Australia, and Zurich, Switzerland).

2. Methods

2.1. Model description

The mechanistic urban ecohydrological model Urban Tethys-Chloris (UT&C) is a combination of an urban canyon scheme and an ecohydrological model and it is solving the energy and water budget on a neighbourhood scale (Meili et al., 2020a). UT&C calculates urban air and surface temperatures, air humidity and soil moisture, as well as the urban energy and hydrological fluxes in the absence of snow. UT&C is able to simulate urban tree cover, short ground vegetation, and green roofs taking into account plant biophysical and ecophysiological

characteristics. The model includes the interaction of trees with radiation, tree evapotranspiration, and the tree influence on the aerodynamic roughness and displacement height.

UT&C is especially suited and, therefore, chosen for this study due to its mechanistic representation of plant evapotranspiration, which is often simplified in urban canopy models (e.g. Krayenhoff et al., 2020; Mussetti et al., 2020), and its inclusion of a physical tree structure within the urban canyon that directly interacts with radiation as described below. One further advantage of UT&C, compared to other models (e.g. Manickathan et al., 2018), is its low computational demand, which allows to run multiple scenarios at an hourly time step for the duration of a year (or longer) thus facilitating analysis on diurnal and seasonal timescales.

UT&C assumes an infinite two-dimensional urban canyon with two uniform rows of street trees that interact with direct shortwave radiation through shadow cast and with diffuse shortwave and longwave radiation through the modification of sky-view factors. The model calculates infinite shortwave and longwave radiation reflections within the urban canyon including tree crowns using reciprocal view factors between the surfaces, and the surfaces and the sky. Sky-view factors and surface-view factors are calculated with a Monte-Carlo ray tracing algorithm. Tree transmissivity for direct shortwave radiation is calculated as a function of leaf area index (LAI) and an optical transmissivity coefficient (Meili et al., 2020b). However, it is not accounted for in the view factor calculation used in the diffuse radiation exchange. Note, that this can potentially overemphasize longwave radiation trapping at night. Furthermore, UT&C does not account for radiation effects at street crossings.

Transpiration of trees and short ground vegetation, e.g. grass, is simulated with a biochemical model of photosynthesis taking into account environmental factors such as photosynthetic active radiation, vapour pressure deficit, and soil moisture accessed by plant roots. Transpiration is calculated separately for sunlit and shaded canopy fractions which are modelled as a function of LAI and a simplified optical transmissivity of the canopy (Meili et al., 2020b). Interception of water on the vegetation canopy is modelled with a mass budget approach following the Rutter model (Rutter et al., 1971, 1975; Ivanov et al., 2008; Fatichi et al., 2012a, 2012b). After rain events, vegetation canopies are partially water covered and evaporation from interception is calculated for the water covered canopy fraction, while transpiration is calculated for the dry canopy fraction. Water covered and dry canopy fractions are calculated according to Deardorff (1978). In all the simulations of this study, vegetation is well watered, in order to ensure that no water stress occurs as to quantify the maximum possible tree evapotranspiration effects.

UT&C calculates aerodynamic roughness and displacement heights according to the parametrizations of Kent et al. (2017) for staggered arrays, which include the effects of trees in the turbulent exchange of energy in urban canyons. The inclusion of a dense and short tree canopy within an urban canyon can smooth the overall city structure and therefore, reduce urban roughness leading to a reduction of energy exchange efficiency from within the urban canyon to the atmosphere, while tall trees can cause the opposite effect (Giometto et al., 2017; Kent et al., 2017). The wind profile is parametrized using the aforementioned urban roughness and displacement heights (Macdonald et al., 1998; Kent et al., 2017). However, the current version of UT&C does not include wind blockage by trees within the urban canyon. Furthermore, the bulk parameterization of UT&C does not allow to calculate the alteration of the three dimensional wind field within the urban canyon due to trees as could be done with computational fluid dynamics models, such as the one presented by Manickathan et al. (2018). Hence, wind blockage and three dimensional wind effects are not analysed. Note, that simplifications such as this, as well as the two-dimensional radiation geometry reduce the computational demand and allow for the aforementioned analysis of multi-year time spans.

UT&C is currently not coupled to a mesoscale meteorological model

such as the Consortium for Small-scale Modelling (COSMO) (Rockel et al., 2008; Mussetti et al., 2020) or the Weather Research and Forecasting model (WRF) (Skamarock et al., 2008; Wang et al., 2018), and we force the model with hourly meteorological data over the period of one year for each selected city (Sect. 2.3). Hence, the results analyse the local tree effects on the urban canopy layer air temperatures and surface temperature but do not account for the mesoscale feedbacks. The full technical description of UT&C can be found in Meili et al. (2020a) and the accompanying technical reference material (Meili et al., 2020b).

2.2. Numerical experiments

UT&C accounts for the interaction of urban trees with radiation (Rad), tree transpiration (T) and evaporation from intercepted water on the tree canopy (E) summarized as evapotranspiration (E + T = ET). It further accounts for the influence of the tree structure on the urban aerodynamic roughness, which influences the wind profile and the turbulent exchange of energy (WT).

A set of five experimental scenarios (Table 2) were designed to partition the aforementioned tree effects on air and surface temperatures and energy fluxes. Scenario A includes all the combined effects of trees (Rad + ET + WT) on urban climate. Scenarios B, C, and D use the same urban geometry and material/vegetation parameters as scenario A (see Sect. 2.3) but some processes are switched off to isolate the different tree effects. Specifically, tree evapotranspiration is switched off (ET = 0) in scenario B; the effects of the tree structure on the urban roughness is excluded in scenario C, and in scenario D, both tree evapotranspiration and trees' roughness alteration are omitted, only accounting for interactions between tree structure and radiation. Finally, scenario E represents the same urban set-up as A–D, but without tree cover to eliminate any tree effect. Note, a scenario including tree evapotranspiration and roughness effects but excluding the tree radiation interactions is omitted on purpose. Such a scenario would violate the energy budget as tree transpiration uses radiation energy, which simultaneously would also reach the ground, if tree structural effects on radiation were excluded. Furthermore, note, that while tree evapotranspiration is turned off in certain scenarios, the evapotranspiration from grass underneath the tree cover, and soil evaporation are kept active in all scenarios and 55 % of the ground area within the canyon is assumed grass covered (Table S2).

The individual tree effects (Rad, ET, WT) can be calculated subtracting the results of the different scenarios as summarized in Table 3. For example, the total effect of tree cover on the urban climate is calculated by subtracting the results of scenario E (urban canyon without trees) from the results of scenario A (urban canyon with trees), while the impact of tree evapotranspiration is quantified by subtracting the results of scenario B (tree without ET) from the results of scenario A (all three effects included). As shown in Table 3, the effects of tree evapotranspiration and urban roughness alteration can be also calculated subtracting different scenarios (i.e., C—D and B—D). These additional options are used to verify that the identification of individual effects does not differ significantly when different simulations are considered, which is indeed confirmed (not shown here). Furthermore, the individual tree effects are likely not completely additive as there is

Table 2

Simulation scenarios to partition the tree-radiation (Rad), tree evapotranspiration (ET), and urban aerodynamic roughness alteration effects of trees (WT) on the urban microclimate and energy fluxes. All scenarios refer to a compact low-rise local climate zone (LCZ3) (Stewart and Oke, 2012) as described in Sect. 2.3.

Scenario	Description	Tree processes considered		
A	LCZ 3 with Trees	Rad	WT	ET
B	LCZ 3 with (Tree – ET)	Rad	WT	
C	LCZ 3 with (Tree – WT)	Rad		ET
D	LCZ 3 with (Tree – ET – WT)	Rad		
E	LCZ 3 no Tree			

Table 3

Calculation of total tree effects (ET + WT + Rad), tree evapotranspiration effects (ET), urban roughness alteration effects by trees (WT), and tree-radiation effects (Rad) on the urban canopy-layer climate by subtracting simulations of scenarios A to E. Table 2 describes the corresponding simulation set-up of scenario A to E.
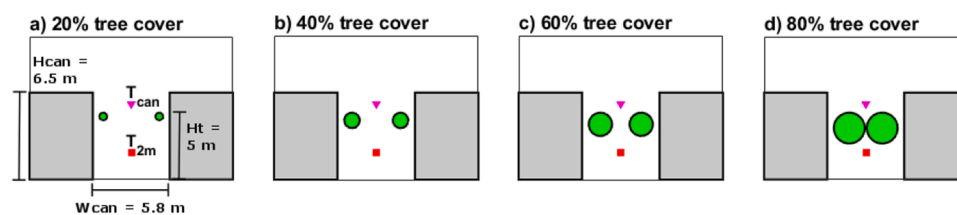
Modification due to	First Option	Second Option
Tree (ET + WT + Rad)	A - E	
Tree evapotranspiration (ET)	A - B	C - D
Urban roughness alteration caused by tree structure (WT)	A - C	B - D
Tree-radiation interaction (Rad)	D - E	

some nonlinear coupling and interactions among them. For example, a highly transpiring tree canopy will be cooler than a non-transpiring one and therefore, might interact differently in the urban energy exchange. To check the magnitude of these nonlinearities, the three single effects are summed up and compared to the total tree effect in Fig. 2.

2.3. Urban characteristics and climate

The radiation, evapotranspiration, and urban roughness effects associated to urban trees are analysed for a compact low rise urban setting, which is defined using representative values of local climate zone 3 (LCZ3) according to Stewart and Oke (2012). The tree effects are analysed for 20 %, 40 %, 60 %, and 80 % tree plan area fraction within the canyon with temporally constant LAI for Phoenix, Singapore, and Melbourne, and seasonally varying LAI for Zurich (Table SI5). Tree LAI refers to the leaf area per ground area immediately underneath the tree canopy. LAI is assumed identical in all the four tree cover fraction scenarios, i.e., only the planar tree cover extent changes but not the canopy thickness. The height of the tree's top is kept constant, as well as the distance between tree's crown and nearest wall. The urban and tree geometry is illustrated in Fig. 1. The urban geometry, material, soil, interception, and site specific vegetation parameters, as well as the anthropogenic heat input, are summarized in Tables SI2 - SI6. Street orientation is chosen to be east-west. We also analysed the north-south orientation for each scenario, but these showed only minor differences in the results and are thus not further discussed (Figure SI3). A tree cover of 80 % within the canyon might not be a realistic scenario, but it is chosen to illustrate the maximum potential effects that could be expected.
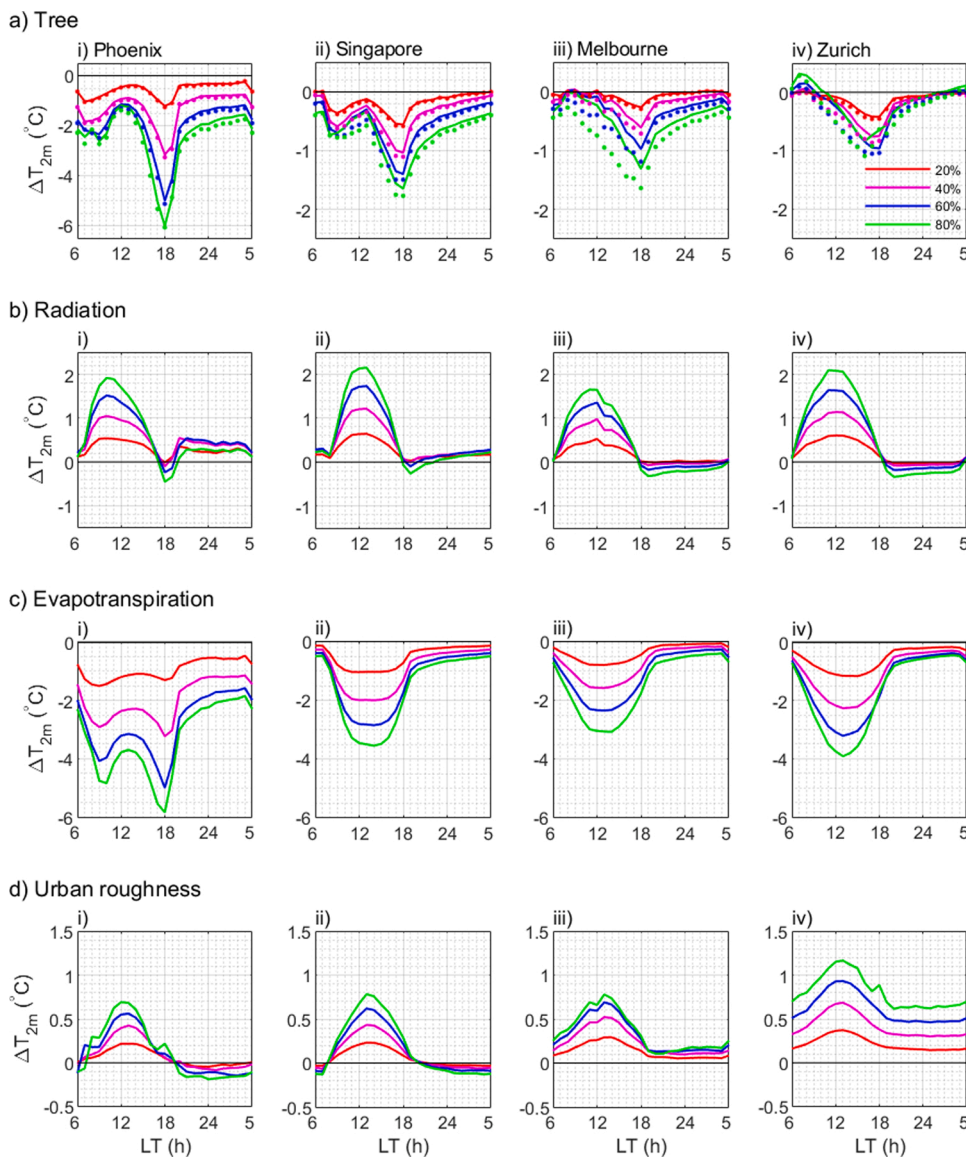
The tree effects are analysed in four cities with distinctively different climates: Phoenix, Singapore, Melbourne, and Zurich over the period of one year. To specify the background climatic forcing, UT&C requires meteorological input time series above building height, which were present in Phoenix, Singapore, and Melbourne. The meteorological input forcing in Zurich was measured at 2 m height (10 m for wind speed) (Mussetti et al., 2019), which introduces a degree of uncertainty in the absolute simulated air temperature at 2 m height in the Zurich scenario. Direct and diffuse shortwave radiation, longwave radiation, air temperature, humidity, wind speed, precipitation, and air pressure measured at meteorological stations, which are described in the following, are used for the purpose of model forcing.

Phoenix experiences a hot arid subtropical desert climate (Köppen classification: BWh) with very high summer temperatures and cooler winter temperatures (Chow et al., 2014). Relative humidity is low as well as the yearly precipitation amount, namely 101 mm y^{-1} during the one-year simulation period. The meteorological data used to force the model simulations for Phoenix were measured in the suburb of Maryvale (33° 29′ 2″ N, 112° 8′ 35″ W, 337 m a.s.l.), which is classified as an "open low rise" local climate zone (LCZ6) (Chow et al., 2014). Singapore experiences high air temperature, high humidity and abundant rainfall (data mean of 1840 mm y^{-1}) year round typical of a tropical rainforest climate (Köppen classification: Af) (Velasco et al., 2013; Roth et al., 2017). The meteorological data used to force the model simulations for Singapore were measured in Telok Kurau (1° 18′ 51″ N, 103° 54′ 40″ E, 10 m a.s.l.), which is classified as a "compact low rise" local climate zone (LCZ3) (Velasco et al., 2013; Roth et al., 2017). Melbourne has a temperate oceanic climate (Köppen classification: Cfb) (Sturman and Tapper, 2006) with warm summers and mild winters. The yearly rainfall amount is low to moderate with 612 mm y^{-1} during the simulation period. The meteorological data used to force the model simulations in Melbourne was measured in the suburb of Preston (37° 49′ S, 144° 53′ E, ~93 m a.s.l.), which is classified as an "open low rise" local climate zone (LCZ6) (Coutts et al., 2007a, 2007b). Zurich has as a mixture of an oceanic climate (Köppen classification: Cfb) and a humid continental climate (Köppen classification: Dfb) with four distinct seasons (Mussetti et al., 2019). The yearly rainfall amount is moderate with 1287 mm y^{-1} during the simulation period. The meteorological data used to force the model simulations in Zurich was measured in the city district Fluntern by the Swiss meteorological services (47° 22′48″ N, 8° 34′12″ E, 556 m a.s.l., Meteo Swiss, 2020), which is classified as an open low rise zone (LCZ 6) (Mussetti et al., 2019). The detailed description of the meteorological measurement campaign in Maryvale Phoenix can be found in Chow et al. (2014), in Telok Kurau Singapore in Velasco et al. (2013) and Roth et al. (2017), and in Preston Melbourne in Coutts et al. (2007a, 2007b). The total simulation period in each location is one year at hourly time steps with meteorological data from mid Dec. 2011 to mid Dec. 2012 in Phoenix, May 2013 to April 2014 in Singapore, mid Aug. 2003 to mid Aug. 2004 in Melbourne, and the year 1981 in Zurich.

The UT&C model performance was previously assessed with tower based eddy-covariance measurements using the same meteorological forcing data as described above in Phoenix, Singapore, and Melbourne in low rise urban climate zones (LCZ3 and LCZ6, see above). The model evaluation, presented in Meili et al. (2020a), showed agreement between simulations and measurements, with metrics of performance in line or better than other modelling studies for these locations (e.g., Grimmond et al., 2011; Demuzere et al., 2017; Harshan et al., 2017; Nice et al., 2018). Specifically, coefficients of determination (R^2) were >0.99 for net radiation in all three sites. R^2 was 0.94, 0.90, and 0.92 for sensible heat, and 0.60, 0.62, and 0.50 for latent heat in Singapore, Melbourne, and Phoenix, respectively (Meili et al., 2020a). Root mean square errors (RMSE) were 20.8, 9.5, and 12.5 Wm^{-2} for net radiation, 23.5, 36.6, 27.4 Wm^{-2} for sensible heat, and 28.1, 26.8, and 19.5 Wm^{-2} for latent heat in Singapore, Melbourne, and Phoenix, respectively (Meili et al., 2020a). UT&C has not been compared against

Fig. 1. Modelled urban geometry with a) 20 %, b) 40 %, c) 60 %, and d) 80 % tree cover within the urban canyon of a compact low-rise residential neighbourhood (LCZ3). T_{2m} denotes the location of the 2 m air temperature and T_{can} the location of the air temperature at the canyon displacement height plus canyon roughness length ($h_{disp,can} + z_{0,m,can}$), which happens to be above the tree canopy. Hcan denotes the canyon height, Wcan the canyon width, and Ht the tree canopy height.

Fig. 2. Change in 2 m air temperature ΔT_{2m} across the average diurnal cycle calculated over the warm period in each city (Sect. 2.4) caused by a) urban tree canopy including all effects (A - E), b) only radiation effects (D – E), c) only evapotranspiration effects (A – B), and d) only urban roughness alteration effects induced by trees (A – C) for 20 %, 40 %, 60 %, and 80 % tree cover within the urban canyon in i) Phoenix, ii) Singapore, iii) Melbourne, and iv) Zurich. Dots in a) display the sum of the effects in b), c), and d) while solid lines display the results of simulation A - E. The analysis refers to the 3 hottest months for Phoenix, Melbourne, and Zurich and the whole year for Singapore including all weather conditions that occurred during the specified time period.

measurements in Zurich due to the lack of flux tower data. However, the hydrological and vegetation processes implemented in UT&C are based on the ecohydrological model Tethys-Chloris (T&C) (Fatichi et al., 2012a, 2012b), which has been validated in many studies before (e.g., Paschalis et al., 2015; Mastrotheodoros et al., 2017; Manoli et al., 2018; Marchionni et al., 2020) including for Swiss lowland climate and biomes (Fatichi et al., 2014).

2.4. Analysis

First, the tree-radiation, evapotranspiration, and urban roughness effects caused by urban trees are individually quantified for the three hottest months of the year in Phoenix and Zurich (June to August), and Melbourne (December to February), and for the whole year in Singapore (Sect. 3.1). The three hottest months are selected for Phoenix, Melbourne, and Zurich as this is likely the time period when cooling is most needed, and the radiation and evapotranspiration effects are, a priori, expected to be largest. The complete one-year period is analysed in Singapore due to its low intra-annual climate variability with continuous high air temperature and humidity (Sect. 2.3). The magnitude of the effects along the diurnal course is analysed through changes of 2 m air temperature (ΔT_{2m}) below the tree canopy, changes of air temperature at a reference canyon height (ΔT_{can}) above the tree canopy (i.e., the displacement height plus roughness length ($h_{disp,can} + z_{0,m,can}$), Table SI1), and changes of area averaged wall and ground surface temperature ($\Delta T_{s,ave}$). The location of T_{2m} and T_{can} are displayed in Fig. 1. The location of T_{can} changes slightly with tree cover amount due to changes in $h_{disp,can}$ and $z_{0,m,can}$, but the differences in $h_{disp,can} + z_{0,m,can}$ are minimal (Table SI1). Furthermore, the energy exchange between the canyon and the overlying atmosphere, the integrated surface energy fluxes, and the aerodynamic and stomatal resistances are analysed to explain the physical mechanisms underlying the various effects.

Second, the seasonal and diurnal impact of trees on T_{2m} is analysed to determine the role of climatic differences on the expected tree benefits (Sect. 3.2) using the full simulation year, with the exception of time steps with atmospheric forcing temperature T_{atm} below 5 °C as the current version of UT&C does not include snow conditions. Furthermore, only time periods with a LAI larger than 0.5 are used in Zurich, where LAI varies seasonally as to avoid completely defoliated trees due to model limitations in handling radiation transmission in these conditions (Sect. 2.1).

Third, the distribution of ΔT_{2m} is analysed using only hourly values for periods with air temperature higher than a given threshold to determine the cooling potential of trees at peak temperatures (Sect. 3.3).

The threshold for high air temperature is determined as the 90th percentile of T_{2m} in an urban canyon without trees considering the entire year at hourly time steps (Scenario E), hence, selecting the 10 % hottest hours for each city. Specifically, the temperature thresholds $T_{2m,90th}$ are $T_{2m} > 38.8$ °C in Phoenix, $T_{2m} > 33.7$ °C in Singapore, $T_{2m} > 22.8$ °C in Melbourne, and $T_{2m} > 22.3$ °C in Zurich.

3. Results

3.1. Radiation, evapotranspiration, and urban roughness effects during the warm period

The tree effects on 2 m air temperature T_{2m} during the warm period (3 hottest months for Phoenix, Melbourne, and Zurich and the whole year for Singapore) depends on climate, time of the day, and tree cover extent as displayed in Fig. 2. The simulations show a similar diurnal profile of ΔT_{2m} in Phoenix and Singapore with two cooling peaks, one during the early morning and the other during the late afternoon hours, while Melbourne and Zurich only exhibit a single cooling peak in the late afternoon hours (Fig. 2a).

During daytime, the highest T_{2m} cooling occurs in Phoenix at 1800 local time (LT) with 1.2 °C and 6.0 °C for 20 % and 80 % tree cover, respectively, in the absence of soil moisture limitations, while a smaller cooling peak is seen at 0700/0900 LT with 1 °C and 2.6 °C for 20 % and 80 % tree cover. In Singapore, a similar diurnal pattern is found with highest cooling of T_{2m} at 1800 LT (0.6 °C and 1.6 °C for 20 % and 80 % tree cover) and a smaller cooling peak at 0900/0800 LT (0.4 °C and 0.7 °C for 20 % and 80 % tree cover). The limited or non-existent cooling effect of trees during midday in hot climates, such as Phoenix and Singapore, can be explained by the decreasing or plateauing transpirative cooling (Fig. 2c) when warming effects caused by radiation and a smoother city structure are high (Fig. 2b and d), as explained in the following sections. Melbourne and Zurich only experience one peak cooling with a T_{2m} decrease of 0.3 °C and 1.3 °C at 1800 LT, and 0.4 °C and 0.8 °C at 1800/1600 LT for 20 % and 80 % tree cover, respectively.

During night time, a high tree cover extent lowers T_{2m} in Phoenix on average by 0.4 °C and 1.8 °C (20 % and 80 % tree cover), in Singapore by 0 °C and 0.5 °C, and in Melbourne by 0 °C and 0.3 °C between midnight and 0600 LT. The effects in Zurich are neutral with an average cooling or warming of < 0.1 °C for 20 % and 80 % tree cover (Fig. 2a).

These distinct diurnal patterns of ΔT_{2m} associated with the presence of trees in different climates can be explained by a combination of various effects as detailed in the following for daytime and night time separately.

3.1.1. Daytime effects on T_{2m}, T_{can} and $T_{s,ave}$

During daytime, the tree-radiation interaction, including short and long-wave radiation, increases air temperature T_{2m} in all four climates with a higher increase at higher tree cover (Fig. 2b, Sect. 3.1.3). The magnitude of the maximum T_{2m} increase due to the radiation is similar in Phoenix, Singapore, and Zurich with 0.5 °C, 0.6 °C, and 0.6 °C for 20 % tree cover and 1.9 °C, 2.1 °C, and 2.1 °C for 80 % tree cover, respectively, while the maximum increase in T_{2m} in Melbourne is slightly smaller at high tree cover with 0.5 °C and 1.6 °C for 20 % and 80 % tree cover.

Tree evapotranspiration cools T_{2m} in all analysed climates with a higher decrease at higher tree cover (Fig. 2c, Sect. 3.1.4). The maximum decrease in T_{2m} is 1.5 °C, 1.0 °C, 0.8 °C, and 1.2 °C for 20 % tree cover, and 5.8 °C, 3.6 °C, 3.1 °C, and 3.9 °C for 80 % tree cover in Phoenix, Singapore, Melbourne, and Zurich, respectively. Furthermore, the magnitude of T_{2m} decrease is remarkably similar during midday in all four climates. Such a similar ΔT_{2m} is caused by high vapour pressure deficits in hot and dry cities, such as Phoenix, that lead to stomatal closure and limited transpiration rates during the hottest hours of the day as explained in Sect. 3.1.4. Note that, due to the full irrigation of vegetation, soil moisture is not a limiting factor for transpiration in this study.

The decrease in aerodynamic roughness due to the presence of a dense tree canopy shorter than building height increases T_{2m} during daytime in all analysed climates with a higher increase at higher tree cover (Fig. 2d, Sect. 3.1.5). The highest T_{2m} increase with 0.4 °C and 1.2 °C for 20 % and 80 % tree cover is modelled in Zurich as a consequence of calm winds and fully developed canopies with an average LAI of 4.9 from June to August. Phoenix, Singapore, and Melbourne experience a maximum T_{2m} increase of 0.2 °C, 0.2 °C, and 0.3 °C for 20 % tree cover, and 0.7 °C, 0.8 °C, and 0.8 °C for 80 % tree cover, respectively.

Adding the tree-radiation, evapotranspiration, and urban roughness effects results in the distinct diurnal pattern of ΔT_{2m} as presented in Fig. 2a. Similar effects of urban trees on the diurnal pattern of ΔT_{can} are also simulated above the tree canopy although with a slightly different magnitude (Fig. SI1a).

The simple sum of the three effects caused by urban trees (dots in Fig. 2a) add up almost linearly to the overall effect of urban trees (solid line in Fig. 2a). There are, however, some small differences due to nonlinear interactions among the effects, but these are less relevant than the three individual effects.

The highest daytime cooling of $T_{s,ave}$ is modelled in Phoenix with 1.7 °C and 6.5 °C at 20 and 80 % tree cover, while Singapore experiences 0.9 °C and 3.3 °C, Melbourne 1.1 °C and 3.9 °C, and Zurich 0.9 °C and 3.2 °C cooling at 20 % and 80 % tree cover (Fig. SI2a). The most striking difference between tree effects on air (T_{2m}, T_{can}) vs surface temperature ($T_{s,ave}$) are the radiation effects. While the tree radiation interaction results in warmer air temperature during daytime, it provides the highest surface temperature $T_{s,ave}$ cooling continuously from midday to late afternoon with a higher $T_{s,ave}$ decrease at higher tree cover (Fig. SI2b). Shading cools the urban surface during daytime, which overcomes the other tree induced radiation effects such, as radiation trapping (Sect. 3.1.3).

3.1.2. Night time effects on T_{2m}, T_{can} and $T_{s,ave}$

At night time, a neutral to moderate tree cooling effect on T_{2m} and $T_{s,ave}$ is found with higher temperature decrease at higher tree cover in Phoenix, Singapore, and Melbourne, but not in Zurich where high tree cover can lead to a neutral effect ($T_{s,ave}$) or slightly increase temperature (T_{2m}) (Figs. 2a and SI2a). In Zurich, the aerodynamic roughness alteration effects on T_{2m}, T_{can}, and $T_{s,ave}$ are particularly significant throughout the night, which leads to the mentioned neutral to warming effects at high tree cover. On average, radiation and evapotranspiration effects of trees are small during the night due to the absence of solar shortwave radiation, which is the major (but not only) forcing for radiation effects. The effect of urban roughness alteration by trees depends on the magnitude of wind speed and the tree canopy structure. Hence, its effect can still be substantial during night time at high tree cover as modelled in Zurich (T_{2m}, T_{can}, $T_{s,ave}$). In Phoenix, high vapour pressure deficits at night lead to a non-negligible nocturnal transpiration and temperature reduction. Transpiration occurs from leaf cuticular conductance and imperfect stomatal closure as explained in the following sections.

3.1.3. Mechanistic interpretation of tree-canopy radiation interaction

During daytime, the tree canopy provides shade and, as expected, decreases surface temperature $T_{s,ave}$ in all analysed climates (Fig. SI2b) due to a decrease in absorbed shortwave radiation by the shaded surfaces (Fig. SI4a). At night and with low tree cover, the tree-radiation interaction increases $T_{s,ave}$ in all four climates as sky-view factors (SVF) are reduced by tree canopies, which leads to radiation trapping within the urban canyon and an increase in absorbed longwave radiation across the surfaces (Figs. SI4b and SI4c). This effect is present throughout the diurnal cycle, but during daytime, the shade provision by the tree canopy overcomes the radiation trapping. With high tree cover and dense tree canopies, surface cooling is prolonged into the night as seen in Zurich (Fig. SI2b). Lower daytime $T_{s,ave}$ reduces soil

temperature and heat storage in the ground which counteracts the radiation trapping effect. In summary, the tree-radiation interaction cools $T_{s,ave}$ during day time but increases $T_{s,ave}$ during the night except at high tree cover and dense canopies.

Canopy radiation effects alone result in an increase of T_{2m} and T_{can} in all modelled climates during day time with a higher increase at higher tree cover (Figs. 2b and SI1b). This increase in air temperature is explained by three effects (Fig. 3a). First, the tree structure increases the overall absorbed shortwave radiation within the canopy due to radiation trapping (Song and Wang, 2015) (Fig. SI5a), thus increasing the energy available within the canopy. Second, the tree canopy shades the underlying ground vegetation, thus decreasing the radiation available for transpiration and therefore, the latent heat released by such vegetation (Fig. SI5a). This effect is particularly pronounced in the presented simulations, as more than 50 % of the canyon ground is vegetated (Table SI2). A scenario without vegetated ground was also modelled, which showed a slightly lower increase in T_{2m} and T_{can} during daytime as no transpiration decrease occurred. Third, the inclusion of a non-transpiring, warm tree surface releases a high amount of sensible heat. These three mechanisms combined increase the total sensible heat flux released in the canyon, even though the sensible heat fluxes released by the ground and wall are smaller (Fig. SI5c). The air within the canyon is typically unstable during day time with low median aerodynamic resistance and the increase in sensible heat raises both T_{can} and T_{2m}. At night, the tree-radiation effects on T_{2m} vary with climate with an air temperature increase in Phoenix and Singapore, and a decrease in Melbourne and Zurich.

3.1.4. Mechanistic interpretation of tree evapotranspiration effects

Tree evapotranspiration leads to a decrease in T_{2m}, and T_{can} (Fig. 2c,

and SI1c) throughout the entire day and in all four climates with higher cooling effects at higher tree cover. As the amount of solar radiation received by the urban surfaces does not change, the decrease in T_{2m}, and T_{can} also indirectly decreases $T_{s,ave}$ in all four climates (SI2c). The evapotranspirative cooling effect is mostly caused by the shift in energy partitioning from sensible to latent heat of well-watered vegetation, which is seen in the decrease/increase of canyon sensible/latent heat (Fig. 3b and Fig. SI6). The highest cooling effect is modelled at times of high transpiration rates, which do not necessarily occur at the peak of absorbed solar radiation. In fact, high air temperatures in dry climates and the reduced amount of vegetation in cities can lead to a high vapour pressure deficit (VPD) that triggers a physiological reaction leading to stomatal closure (Morison and Gifford, 1983; Oren et al., 1999) (Fig. SI7). Hence, limited evapotranspirative cooling effects are found during midday in Phoenix. Tree evapotranspiration also provides a night time cooling effect due to residual stomatal conductance (Caird et al., 2007), which allows some water loss from the leaves even when stomata are mostly closed. This is especially relevant in cities with a high VPD at night, such as in Phoenix (Fig. 2ci).

3.1.5. Mechanistic interpretation of the aerodynamic roughness alteration effects of trees

In the analysed scenarios, trees within the urban canyon increase the smoothness of the city fabric (decrease in urban roughness, $z_{0,m,can}$, Table SI1), which increases the aerodynamic resistance and reduces the turbulent exchange from canyon air to the atmospheric forcing level $r_{ah,can \to atm}$ (Fig. 3c and Fig. SI9). The increase in $r_{ah,can \to atm}$ leads to an increase in T_{can} throughout the day and night, an increase proportional to the tree cover amount (Fig. SI1d). Similarly, T_{2m} and $T_{s,ave}$ increase during daytime due to roughness effects (Fig. 2d and SI2d) as the air
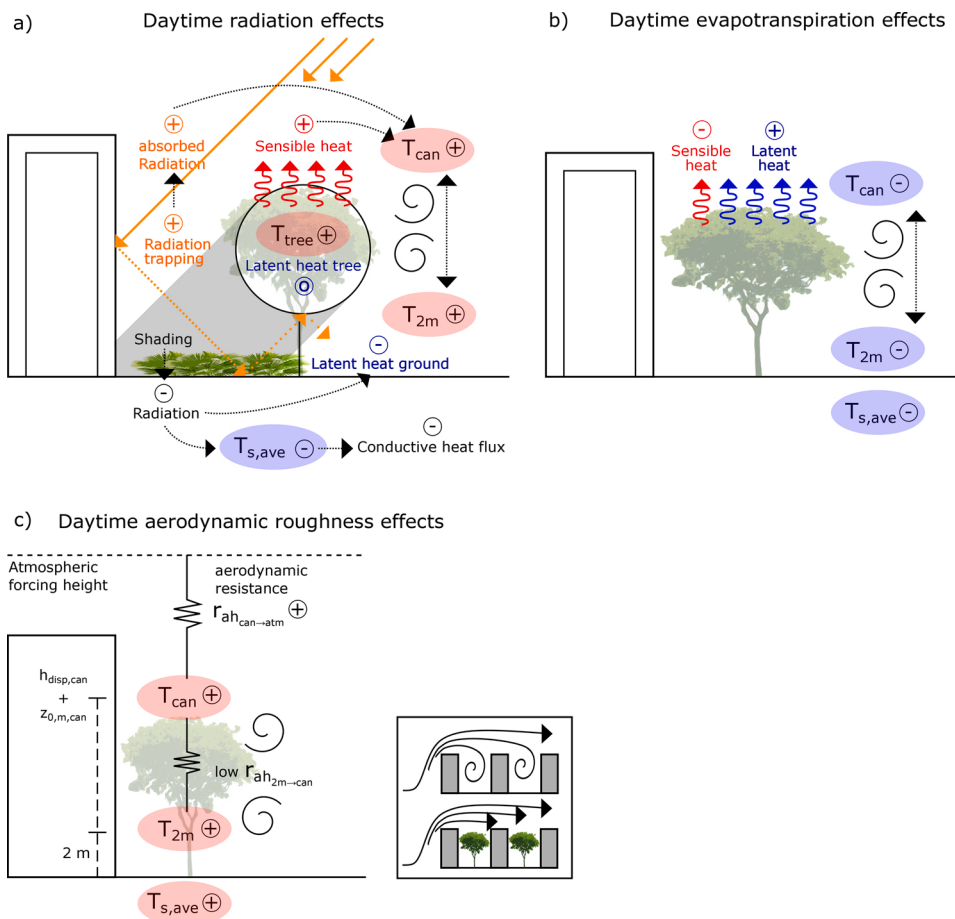

Fig. 3. Representation of the main mechanisms that alter 2 m air temperature (T_{2m}), air temperature above the tree canopy (T_{can}), and average surface temperatures ($T_{s,ave}$) when only considering a) daytime tree-radiation interaction, b) daytime tree evapotranspiration, and c) daytime aerodynamic roughness alterations caused by urban trees. T_{tree} denotes the tree surface temperature, $h_{disp,can}$ the canyon displacement height, $z_{0,m,can}$ the aerodynamic urban roughness, and $r_{ah,2m \to can}$ and $r_{ah,can \to atm}$ the aerodynamic resistance from 2 m height to reference canyon height and from reference canyon height to atmospheric forcing height, respectively. The +, -, and 0 sign denote an increase, a decrease, and no change in energy flux or temperature.

column within the canyon is simulated to be unstable with low aerodynamic resistance $r_{ah,2m \to can}$ (Fig. SI10b), and the increase in $r_{ah,can \to atm}$ tends to keep the heat released by hot urban surfaces within the canyon, thus increasing temperatures.

At night, the urban roughness alteration effects of trees on T_{2m} and $T_{s,ave}$ vary, likely due to differences in the simulated atmospheric stability within the canyon. In these simulations, Phoenix and Singapore are characterized by stable atmospheric conditions with high $r_{ah,2m \to can}$ at night, while Melbourne and Zurich exhibit unstable conditions with low $r_{ah,2m \to can}$ (Fig. SI10b). Due to high values of $r_{ah,2m \to can}$, the change in T_{2m} in Singapore and Phoenix is most closely linked to $\Delta T_{w,ave}$. As $T_{w,ave}$ gets cooler at night, T_{2m} also decreases (Fig. 2di and 2dii). In Melbourne and Zurich, our simulations show unstable atmospheric conditions within the canyon. Hence, the increase in $r_{ah,can \to atm}$ increases T_{can}, T_{2m} and $T_{s,ave}$ concurrently. The overall urban temperature increase associated to aerodynamic roughness effects is particularly high in Zurich at all hours due to high values of LAI (average LAI of 4.9 from June to August), which further reduces city roughness. Note that the effects shown here are only caused by the alteration of the overall urban canyon aerodynamic roughness and displacement height due to trees within the canyon, and not by their wind blockage effects, which are not analysed in this study as discussed in the study limitations.

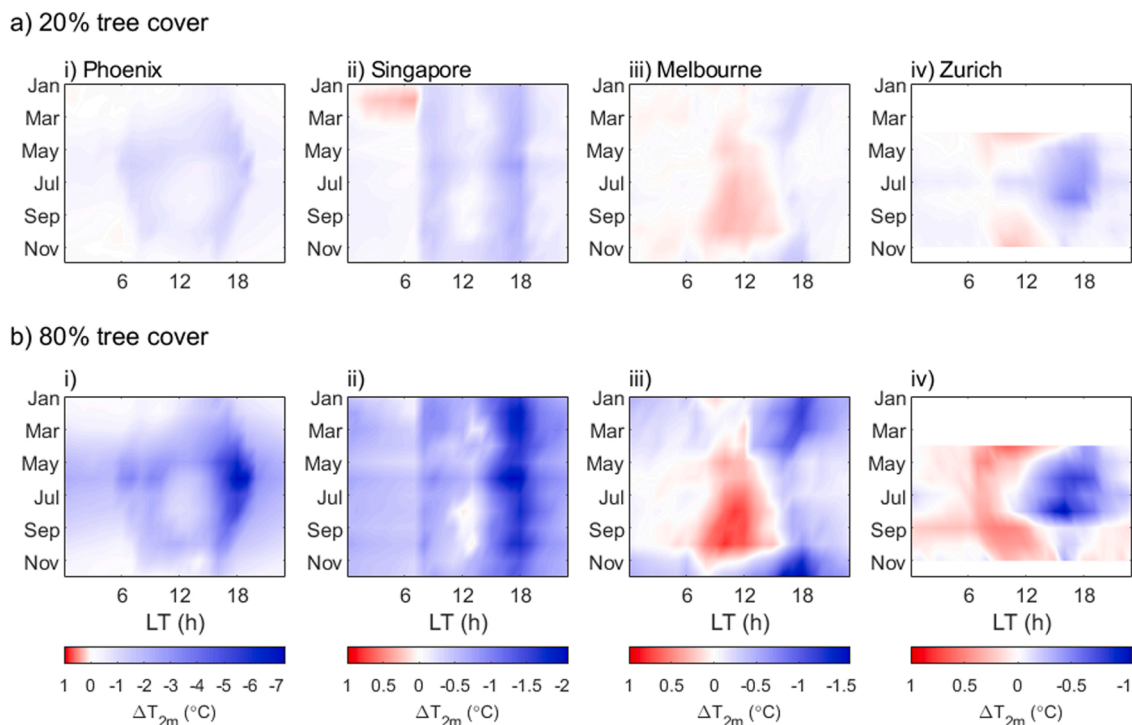### 3.2. Seasonal and diurnal variability of tree effects on 2 m air temperature

In Phoenix, Melbourne, and Zurich, trees generally provide a higher cooling effect on T_{2m} during the warm season (e.g. May to September in Phoenix, November to March in Melbourne, and May to August in Zurich). In cooler seasons (e.g. November to March in Phoenix, and May to September in Melbourne), the T_{2m} cooling by trees is considerably smaller or negligible, and in some cases even warming of T_{2m} is simulated (e.g. during day time from May to September in Melbourne, and October to November in Zurich) (Fig. 4). Differences in ΔT_{2m} are also found throughout the diurnal cycle, but this depends more strongly on the local climate as previously explained (Sect. 3.1).

In Phoenix, the most consistent T_{2m} cooling throughout the entire day is seen in spring as the radiation warming effects during midday and the stomata closure due to high VPD are moderate in this season. The strongest T_{2m} cooling is modelled in summer during the early morning and evening hours in June with 1.2 °C at 0700 LT and 1.7 °C at 1900 LT for 20 % tree cover and 3.4 °C at 0700 LT and 7.3 °C at 1800 LT for 80 %. In summer, cooling is also simulated throughout the night with the highest average night time cooling in June with 0.5 °C for 20 % tree cover and 2.3 °C for 80 % between midnight and 0600 LT. During midday, tree cooling effects become minimal in Phoenix due to high warming rates induced by tree-radiation interactions and stomatal closure caused by extremely high VPD (Sect. 3.1.3 and 3.1.4). In winter, T_{2m} cooling tends to be lowest but is still present during the early morning and late afternoon hours.

Due to its tropical location, Singapore depicts a homogenous cooling effect by trees all year long, and as discussed in Sect. 3.1, experiences the highest T_{2m} cooling during the early morning and late afternoon hours. At night, no T_{2m} changes are simulated, with the exception of an anomalous dry period in February 2014, where an average warming effect of 0.2 °C at low tree cover (20 %) occurs between midnight and 0600 LT, even though vegetation is fully irrigated in our simulations. During midday, tree effects are minimal at low tree cover, while at 80 % tree cover, slight warming effects of 0.1 °C at 1200 LT and 1300 LT are simulated in August, and October. Midday warming is observed during times when direct incoming shortwave radiation is highest (July to October) and/or the relative humidity is high (July to October). Higher incoming shortwave radiation increases the tree-radiation warming effects on T_{2m}, while higher relative humidity in the humid climate of Singapore decreases the cooling effect of tree evapotranspiration.

In Melbourne, low tree cover (20 %) provides minimal T_{2m} cooling with the highest decrease of 0.3 °C found at 1700 LT in December. At high tree cover (80 %), the cooling effects are also highest during summer in the late afternoon hours with a maximum of 1.6 °C at 1800 LT in December and are prolonged throughout the night with an average

Fig. 4. Tree cover effects on 2 m air temperature T_{2m} for a) 20 % and b) 80 % tree cover within the canyon in i) Phoenix, ii) Singapore, iii) Melbourne, and iv) Zurich: the seasonal variability of the diurnal cycle is shown. Winter months in Zurich are not analysed as trees are defoliated during this period (LAI < 0.5). Note the different temperature scales in the four plots.

T_{2m} cooling of 0.4 °C. In winter and spring, T_{2m} warming is simulated during the day, which is highest in July to October with 0.3 °C warming at 1100 LT in August with 20 % tree cover, and 0.8 °C in October at 1000 LT with 80 % tree cover.

In Zurich, the highest cooling effects are simulated in summer during the afternoon and early evening hours with a maximum of 0.5 °C at 1700 LT for 20 % tree cover and 1.1 °C at 1600 LT for 80 % in August. At high tree cover (80 %), warming occurs throughout the year in the morning hours with a maximum of 0.7 °C at 1000 LT in April. At low tree cover (20 %), warming mostly occurs during spring and autumn in the morning hours with a maximum of 0.3 °C at 1100 LT in November.

In summary, trees provide higher cooling in Phoenix, Melbourne, and Zurich during the warm season, while in the cool season, air temperature reduction is less in Phoenix and neutral to increasing air temperatures are simulated in Zurich. As Singapore is continuously hot throughout the year, seasonal changes in the cooling effects are less pronounced.

3.3. Tree effects during the warmest hours

Analysing the effects of trees only for hours where $T_{2m} > T_{2m,90th}$ can change the distribution of ΔT_{2m} with differences across climates.

In Phoenix and with low tree cover (20 %), only small differences are found in the distribution of ΔT_{2m} at peak temperatures. ΔT_{2m} is predominantly negative with most ΔT_{2m} values occurring between 0 to -2 °C (Fig. 5ai). However, at high tree cover (80 %), differences in the distribution of ΔT_{2m} are more apparent. When considering all time steps, the majority of ΔT_{2m} is between 0 to -5 °C, while during the 10 % hottest hours of the year, T_{2m} cooling is more pronounced with a higher percentage of ΔT_{2m} between -5 to -8 °C (Fig. 5bi).

In Singapore, effects vary at low and high tree cover, where the majority of ΔT_{2m} is negative when considering all hours of the year between 0 to -1 °C for 20 % tree cover and 0 to -2.5 °C at 80 % tree cover. However, reducing the analysis to the 10 % hottest hours of the year, T_{2m} warming becomes more frequent (Fig. 5aii and bii). This finding is

consistent with the previous discussion on reduced cooling effects under high VPDs due to stomatal closure as discussed in Sect. 3.1.4.

In Melbourne and Zurich, the tree cover might cool or warm the air considering all hours of the year, especially at 80 % tree cover. Analysing only the 10 % hottest hours of the year, ΔT_{2m} is more often negative, consistent with the predominant cooling effect of vegetation in the warmest summer hours.

4. Discussion

4.1. Urban trees and radiation

The interaction between trees and the radiation fluxes increases daytime air temperature in all the climates analysed here. This daytime T_{2m} increase is explained by an increase in absorbed shortwave radiation within the canyon and the turbulent energy partitioning by the tree canopy. A healthy tree uses the absorbed radiation energy for transpiration, which increases the latent heat at the expense of the sensible heat flux. In the hypothetical case of a non-transpiring tree, as in scenario D here, the tree heats up during daytime and releases a large amount of sensible heat, which increases air temperature (T_{2m} and T_{can}). Similarly, non-transpiring shading devices, often employed in urban areas, can reach high temperatures as shown with thermal imaging by Shashua-Bar et al. (2011) and can also increase the measured air temperature (Shashua-Bar et al., 2009). In addition, shading of lawns underneath the tree reduces the available solar radiation and thus evapotranspiration of ground vegetation as recently reported by Rahman et al. (2019). The simulated decrease in average surface temperature by UT&C due to tree shading is of smaller magnitude than the often reported field observations (e.g., Armson et al., 2013; Middel et al., 2016; Spangenberg et al., 2008) as modelled surface temperatures are averaged over the urban canyon (and therefore, they include some sun exposed surfaces), whereas measurement studies typically analyse the difference between strictly sunlit and strictly shaded areas, which is expected to be much larger. As artificial shade structures are often used in the urban
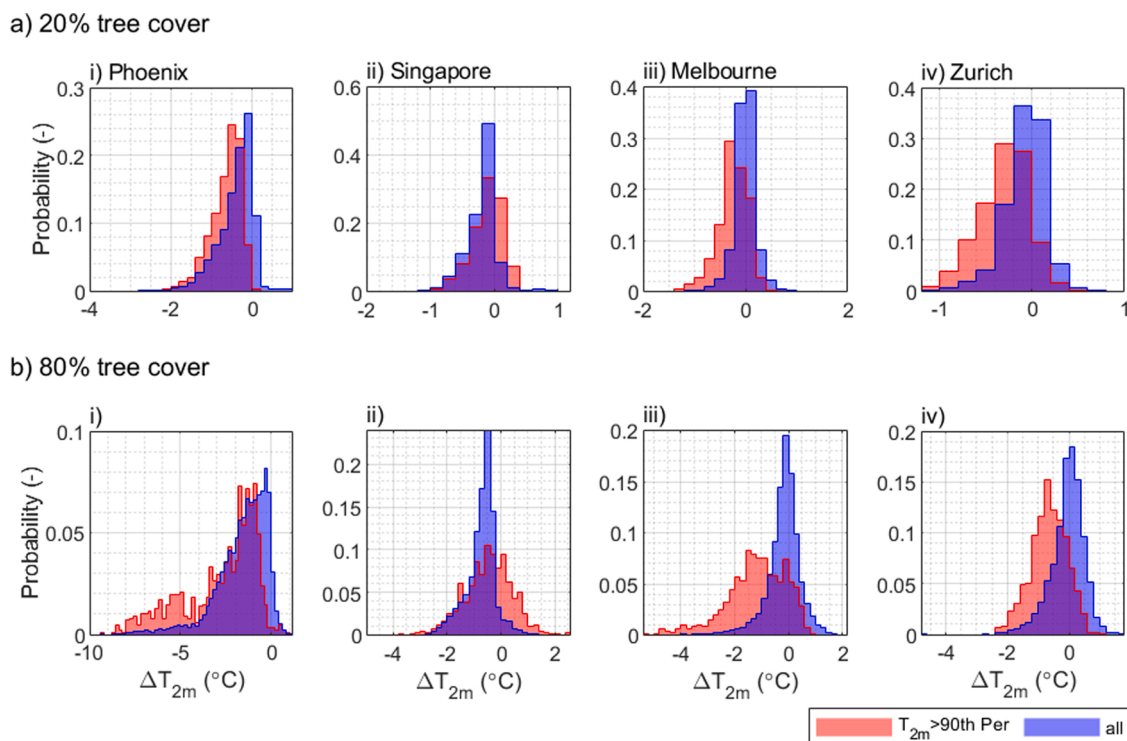

Fig. 5. Distribution of tree cover effects on 2 m air temperature changes ΔT_{2m} for a) 20 % and b) 80 % tree cover within the urban canyon in i) Phoenix, ii) Singapore, iii) Melbourne, and iv) Zurich. The results show distribution of ΔT_{2m} for the whole time series, and the hottest 10 % of all time steps.

environment, future research is needed to determine whether their placement increases the overall canyon air temperature. Note, that the focus of this study lays on air and surface temperatures and not on the outdoor thermal comfort of city dwellers, for which shade provision and therefore, reduction of mean radiant temperature is a key factor with clear beneficial effects in warm environments (Morakinyo and Lam, 2016; Morakinyo et al., 2017).

Previous modelling studies, which quantify the shade effects of urban trees on air temperature, such as Wang et al. (2016) who employed a single layer urban canyon model (Yang et al., 2015), and Upreti et al. (2017) and Wang et al. (2018) who run the coupled WRF and Urban Canopy Model (Skamarock et al., 2008) in Phoenix and throughout the contiguous United States, found a decrease in urban air temperature with the inclusion of tree shade. These apparently contradicting findings are likely related to the way the energy absorbed by the non-transpiring tree surface is treated in the different models. In our simulations of the radiation effects, tree evapotranspiration is set to zero, while the tree canopy still receives the full radiation load and hence, the energy is dissipated through an increase in sensible heat. Only accounting for a decrease in absorbed radiation by ground and wall surfaces would diminish the overall absorbed energy by the urban area, which would decrease air temperature due to lower surface temperatures. However, trees do not use the total amount of absorbed radiative energy for transpiration and the energy partitioning of sensible and latent heat by the tree canopy (Bonan, 2016) is an important factor to consider for accurate microclimatic predictions, especially under unfavourable environmental conditions (e.g. dry and hot), which might limit transpiration as discussed in Sect. 4.2.

The night-time tree radiation interactions depend on canopy cover extent and climate. A high tree foliage cover leads to a large reduction of ground temperature during the day, which prolongs the cooling effects throughout the night, because of the lower heat storage in the soil and buildings as observed in Zurich and also modelled by Upreti et al. (2017). This result highlights that tree shading is not only important to reduce daytime temperature but can also be beneficial at night.

4.2. Urban trees and transpiration

Tree evapotranspiration can provide cooling effects throughout the day and night. However, the UT&C simulations show that high VPD, while being a major driver of evapotranspiration, can also limit transpirative cooling due to partial stomatal closure during the hottest hours of the day. This is a well-documented plant hydraulic regulatory effect (e.g., Morison and Gifford, 1983; Monteith, 1995; Oren et al., 1999; McAdam and Brodribb, 2015), which was also observed in urban field campaigns by Gillner et al. (2017) in Dresden in Germany, and Chen et al. (2011) in Dalian City in Northern China. However, studies also show that plant species well adapted to dry and hot climates can provide enhanced cooling effects when well-watered (Wang et al., 2019). Hence, the presented stomatal response to VPD includes a degree of uncertainty and further research is needed to investigate the adaptability of urban vegetation to high VPD when irrigated. As VPD can be higher in the urban environment due to a lower latent heat flux and higher temperatures than in surrounding rural areas, several studies suggest to choose drought tolerant species to provide optimal urban cooling even during heat and drought events (Gillner et al., 2017; Stratópoulos et al., 2018). More generally, we suggest using plants with an anisohydric behaviour (Klein, 2014; Roman et al., 2015; Meinzer et al., 2016), i.e., plants that lower leaf water potentials and maintain higher transpiration rates, even during low soil moisture conditions or high VPD. These plants might provide a larger cooling potential than isohydric plants that tightly regulate leaf water potential, by closing stomata with increasing VPD, and thus reducing transpiration and urban cooling.

UT&C's modelling results show cooling effects due to tree evapotranspiration at night, in agreement with field observations of urban trees in Gothenburg in Sweden (Konarska et al., 2015, 2016). In dry and

hot cities with high night time VPD, such as Phoenix, this effect can be substantial and worth considering as a night time cooling strategy when selecting tree species with high residual stomatal conductance (Caird et al., 2007; Forster, 2014). Chen et al. (2011) found large differences in night time sap flow in relation to VPD among different tree species in Dalian City in China. Hence, if water for irrigation is available, tree species selection should be considered carefully to ensure maximum nocturnal transpirative cooling in places such as Phoenix or other semiarid climates. Note, while high VPD can lead to stomatal closure during daytime, during night time, stomata are already largely closed and higher VPD results in enhanced evapotranspiration because it increases the vapour flux from leaf cuticular conductance and imperfect stomatal closure (Duursma et al., 2019). In our simulations, vegetation is fully irrigated and we purposely excluded water stress, which could considerably decrease the transpirative cooling effects. Additional considerations, which can limit tree transpiration and are not investigated in this study, are unfavourable urban soil conditions (Ow et al., 2019), as for example due to soil compaction (Rahman et al., 2011, 2019).

4.3. Urban trees and aerodynamic roughness

The addition of a short and dense tree canopy, as in the analysed urban setting (i.e. LCZ 3), decreases the overall city aerodynamic roughness and hinders the turbulent energy exchange (Fig. 3c). Consequently, the canyon air warms up during daytime. The smoothing of the city aerodynamic properties due to the inclusion of trees is not often discussed in the literature but should be considered when analysing strategies of intensive urban tree cover increase, with a stature shorter than average building height. However, if the tree canopy is significantly higher than the average building height, aerodynamic city roughness can increase (Fig. SI8) (Giometto et al., 2017; Kent et al., 2017), a scenario not analysed in this study.

The aerodynamic roughness effects of urban trees in this study are generally smaller than the radiative and evapotranspirative effects, but the real tree-wind interactions are likely underestimated, because wind blockage effects by the tree canopy within the canyon are currently not simulated in UT&C. Recent developments of computational fluid dynamic tools accounting for urban trees can help in better representing and evaluating the magnitude of this effect in future studies (e.g., Moonen et al., 2013; Saneinejad et al., 2014; Manickathan et al., 2018).

4.4. Differences across climates and vegetation selection

Phoenix and Singapore show a pronounced T_{2m} decrease during morning and evening hours compared to midday, which is caused by a reduced transpirative cooling during the hottest hours of the day, when the solar radiation and urban roughness effects are large. This is likely a robust pattern as other studies do not find the highest air temperature reduction around midday when radiation is highest, but rather in the morning or evening hours (e.g., Coutts et al., 2016), which was also modelled in Melbourne and Zurich. UT&C simulations further suggest that differences in ΔT_{2m} at night in different climates or simply in different urban settings or days might be caused by the atmospheric stability within the canyon.

Throughout the year, the UT&C simulations show the highest tree cooling effects in summer and in the transition seasons, while, in colder periods, tree cooling is less or there is even a warming effect on T_{2m}, as in Melbourne and Zurich. Such an air temperature warming during cold periods could be beneficial in temperate regions (Yang and Bou-Zeid, 2018).

In summary, a comprehensive understanding of the individual tree effects leading to the distinct diurnal and seasonal change of ΔT_{2m} can facilitate the selection of appropriate tree species and cover to achieve certain cooling or warming objectives for current and potentially future climatic conditions. As one of the most striking results, limitation to tree evapotranspiration seems to be an important factor in the cooling

potential provided by vegetation, during hot and dry periods. Paradoxically, the warming effect due to tree-radiation interaction of a "non-transpiring tree structure" could be significant during dry periods when tree evapotranspiration is minimal. Hence, cities that will experience longer dry periods and higher temperatures in the future, need to consider in detail physiological and biophysical vegetation aspects together with hydrological budget considerations, as vegetation could produce unwanted detrimental effects on local urban canopy air temperatures.

4.5. Limits of interpretation

A representative low-rise urban set up (LCZ 3) is chosen in this study to analyse the varying tree effects. The magnitude of the single effects is likely to vary with changes in urban density and properties, as well as vegetation structure and traits. For instance, tree height is chosen shorter than building height, which results in a decrease of urban roughness and an increase in daytime air temperature within the urban canopy. Selecting trees that are substantially higher than the surrounding buildings can increase aerodynamic roughness in the applied parameterization (Fig. SI8) (e.g., Giometto et al., 2017; Kent et al., 2017). Currently, wind blockage effects of trees are not considered in the presented results, which simplify the description of turbulent exchanges within the canyon.

More generally, UT&C calculates the turbulent energy exchange based on a simple resistance scheme (Masson, 2000; Wang et al., 2013; Meili et al., 2020a). Recent developments of computational fluid dynamic tools that include urban trees can help in providing a more accurate description of turbulent exchanges, convection efficiency, and buoyancy, and they can potentially validate or disprove the simulated effects, such as the air temperature increase underneath non-transpiring trees or the difference in atmospheric stability under various urban and climate conditions (e.g., Moonen et al., 2013; Saneinejad et al., 2014; Giometto et al., 2017; Manickathan et al., 2018). Additionally, while UT&C has showed satisfactory model performance through comparison of simulated and measured energy fluxes in Phoenix, Singapore, and Melbourne (Meili et al., 2020a), the model has so far not been extensively tested against air and surface temperature measurements. This introduces another degree of uncertainty in the presented results. The magnitude of the effects strongly controlled by aerodynamic resistances and wind profiles might be revised, if future studies would show that the current description of turbulent exchange deviates strongly from reality. In this case, UT&C's parameterizations governing the impacts of trees and buildings on flow and thermal convection could be refined with a parameterization of intermediate complexity, which accounts for within canyon tree effects on turbulent exchanges (e.g., Krayenhoff et al., 2020; Redon et al., 2020). Despite the mentioned simplifications, we still deem important to discuss and present the effects of tree canopies on aerodynamic city roughness, as it is a way through which trees can modify urban climate.

Furthermore, UT&C, run as a stand-alone code, does not include climatic mesoscale feedbacks induced by changes in energy fluxes. Hence, the presented results refer to the tree effects that can be expected at the local scale without any feedback on and from the city-scale climate.

Last, vegetation is irrigated and always well-watered in the four analysed climates. This allows estimating the maximum evapotranspirative effects of trees. However, such a scenario would require a large amount of anthropogenic water input in arid places such as Phoenix, which might not be feasible or desirable to achieve in reality (Wang et al., 2016).

5. Conclusions

This study quantifies the radiation, evapotranspiration, and aerodynamic urban roughness alteration effects caused by well-watered

urban trees on below and above tree canopy air temperature, as well as surface temperatures using process-based modelling. The partitioning of the effects allows explaining contrasting results in observed air temperature modifications by trees for different times of the day, seasons, and background climatic conditions.

Simulations show that tree evapotranspiration can decrease urban canopy layer air temperature in all analysed climates, but the magnitude is limited during the hottest periods, especially in dry climates, as stomatal conductance is severely reduced at high VPD. Concurrently, the sole interaction of the tree canopy with radiation increases the air temperature in all four climates due to an increase in absorbed shortwave radiation, a decrease in latent heat from shaded ground vegetation, and a large release of sensible heat by a hot non-transpiring tree canopy. Finally, the inclusion of a dense tree canopy shorter than the surrounding buildings reduces the aerodynamic roughness of the neighbourhood, which hinders turbulent energy exchange and increases daytime air temperature, especially under calm wind conditions and/or dense (high LAI) tree canopies. Note that, with tall trees, urban aerodynamic roughness would increase in the applied parametrization. Additionally, the wind blockage effects of trees within the urban canyon are not analysed in this study but they might provide additional effects on turbulent exchanges. Urban roughness alterations induced by trees during night time provide different responses according to climates, which are likely caused by differences in atmospheric stability within the canyon.

Combining all tree effects together, results in a distinctive diurnal pattern of urban air temperature modification, namely higher air temperature decrease during either morning or evening hours, or both, compared to midday in warm climates. In other words, trees provide air temperature cooling during the majority of the time but cooling can be limited or even reversed at times of extreme heat. This is due to limited transpirative cooling when radiative warming is large as leaves are hydraulically stressed by high VPD values. This effect could be significant and deserves further research to be assessed in more detail and to evaluate if well-watered urban trees can adapt to high VPD values in comparison to their rural counterparts. Selecting tree species that can cope with high VPD levels is important in hot cities to avoid further warming during heat waves.

Urban trees in temperate cities, such as Melbourne and Zurich, can provide both air temperature warming and cooling. T_{2m} warming is largest during the colder seasons while during the hottest hours of the year T_{2m} is mostly reduced. Hence, in the seasonal context, trees in temperate cities are offering the desired effects.

The distinct diurnal and seasonal pattern of tree-induced air temperature changes in different climates needs to be considered when planning future urban greening scenarios. Despite recognized uncertainties in the parameterization of certain processes, the mechanistic explanations obtained with UT&C as presented in this study, can be used to guide future field campaigns and inform research and urban planning projects aimed at improving local urban canyon temperature using greenery, as well as guide decision makers in selecting appropriate tree species to maximize the desired benefits and minimize potential unwanted counter-effects.

Author contributions

NM and SF designed the study, conducted the analysis, and wrote the manuscript with inputs from GM. MR, EV, AC, and WC collected and shared their meteorological measurements for model forcing. All authors gave comments and contributed to the final version of the manuscript.

Declaration of Competing Interest

The authors declare that they have no conflict of interest.

Acknowledgements

Appendix A. Supplementary data

Supplementary material related to this article can be found, in the online version, at doi:https://doi.org/10.1016/j.ufug.2020.126970.

References

Armson, D., Rahman, M.A., Ennos, A.R., 2013. A comparison of the shading effectiveness of five different street tree species in Manchester, UK. Arboric. Urban For. 39 (4), 157–164.

Berland, A., Shiflett, S.A., Shuster, W.D., Garmestani, A.S., Goddard, H.C., Herrmann, D. L., Hopton, M.E., 2017. The role of trees in urban stormwater management. Landsc. Urban Plan. 162, 167–177. https://doi.org/10.1016/j.landurbplan.2017.02.017.

Bonan, G., 2016. Ecological Climatology. Cambridge University Press. https://doi.org/10.21425/f58433332.

Bowler, D.E., Buyung-Ali, L., Knight, T.M., Pullin, A.S., 2010. Urban greening to cool towns and cities: A systematic review of the empirical evidence. Landsc. Urban Plan. 97 (3), 147–155. https://doi.org/10.1016/j.landurbplan.2010.05.006.

Caird, M.A., Richards, J.H., Donovan, L.A., 2007. Nighttime stomatal conductance and transpiration in C3 and C4 plants. Plant Physiol. 143 (1), 4–10. https://doi.org/10.1104/pp.106.092940.

Chen, L., Zhang, Z., Li, Z., Tang, J., Caldwell, P., Zhang, W., 2011. Biophysical control of whole tree transpiration under an urban environment in Northern China. J. Hydrol. (Amst) 402 (3–4), 388–400. https://doi.org/10.1016/j.jhydrol.2011.03.034.

Chow, W.T.L., Volo, T.J., Vivoni, E.R., Jenerette, G.D., Ruddell, B.L., 2014. Seasonal dynamics of a suburban energy balance in Phoenix, Arizona. Int. J. Climatol. 34 (March), 3863–3880. https://doi.org/10.1002/joc.3947.

Coutts, A.M., Beringer, J., Tapper, N.J., 2007a. Characteristics influencing the variability of urban CO2 fluxes in Melbourne, Australia. Atmos. Environ. 41 (1), 51–62. https://doi.org/10.1016/j.atmosenv.2006.08.030.

Coutts, A.M., Beringer, J., Tapper, N.J., 2007b. Impact of increasing urban density on local climate: spatial and temporal variations in the surface energy balance in Melbourne, Australia. J. Appl. Meteorol. Climatol. 46 (4), 477–493. https://doi.org/10.1175/JAM2462.1.

Coutts, A.M., White, E.C., Tapper, N.J., Beringer, J., Livesley, S.J., 2016. Temperature and human thermal comfort effects of street trees across three contrasting street canyon environments. Theor. Appl. Climatol. 124 (1–2), 55–68. https://doi.org/10.1007/s00704-015-1409-y.

Deardorff, J.W., 1978. Efficient prediction of ground surface temperature and moisture with inclusion of a layer of vegetation. J. Geophys. Res. 83, 1889–1903.

Demuzere, M., Harshan, S., Jaervi, L., Roth, M., Grimmond, C.S.B., Masson, V., Oleson, K.W., Velasco, E., Wouters, H., 2017. Impact of urban canopy models and external parameters on the modelled urban energy balance in a tropical city. Q. J. R. Meteorol. Soc. https://doi.org/10.1002/qj.3028.

Duursma, R.A., Blackman, C.J., Lopéz, R., Martin-StPaul, N.K., Cochard, H., Medlyn, B. E., 2019. On the minimum leaf conductance: its role in models of plant water use, and ecological and environmental controls. New Phytol. 221 (2), 693–705. https://doi.org/10.1111/nph.15395.

Fatichi, S., Ivanov, V.Y., Caporali, E., 2012a. A mechanistic ecohydrological model to investigate complex interactions in cold and warm water-controlled environments: 1. Theoretical framework and plot-scale analysis. J. Adv. Model. Earth Syst. 4, 1–31. https://doi.org/10.1029/2011MS000086.

Fatichi, S., Ivanov, V.Y., Caporali, E., 2012b. A mechanistic ecohydrological model to investigate complex interactions in cold and warm water-controlled environments: 2. Spatiotemporal analyses. J. Adv. Model. Earth Syst. 4, 1–22. https://doi.org/10.1029/2011MS000087.

Fatichi, Simone, Zeeman, M.J., Fuhrer, J., Burlando, P., 2014. Ecohydrological effects of management on subalpine grasslands: from local to catchment scale. Water Resour. Res. 50 (1), 148–164. https://doi.org/10.1002/2013WR014535.

Forster, M.A., 2014. How significant is nocturnal sap flow? Tree Physiol. 34 (7), 757–765. https://doi.org/10.1093/treephys/tpu051.

Fung, C.K.W., Jim, C.Y., 2019. Microclimatic resilience of subtropical woodlands and urban-forest benefits. Urban For. Urban Green. 42 (May), 100–112. https://doi.org/10.1016/j.ufug.2019.05.014.

Gillner, S., Vogt, J., Tharang, A., Dettmann, S., Roloff, A., 2015. Role of street trees in mitigating effects of heat and drought at highly sealed urban sites. Landsc. Urban Plan. 143, 33–42. https://doi.org/10.1016/j.landurbplan.2015.06.005.

Gillner, S., Korn, S., Hofmann, M., Roloff, A., 2017. Contrasting strategies for tree species to cope with heat and dry conditions at urban sites. Urban Ecosyst. 20 (4), 853–865. https://doi.org/10.1007/s11252-016-0636-z.

Giometto, M.G., Christen, A., Egli, P.E., Schmid, M.F., Tooke, R.T., Coops, N.C., Parlange, M.B., 2017. Effects of trees on mean wind, turbulence and momentum exchange within and above a real urban environment. Adv. Water Resour. 106, 154–168. https://doi.org/10.1016/j.advwatres.2017.06.018.

Grimm, N.B., Faeth, S.H., Golubiewski, N.E., Redman, C.L., Wu, J., Bai, X., Briggs, J.M., 2008. Global change and the ecology of cities. Science 319 (February).

Grimmond, C.S.B., Blackett, M., Best, M.J., Baik, J., Belcher, S.E., Beringer, J., Bohnenstengel, S.I., Calmet, I., Chen, F., Coutts, A., Dandou, A., Fortuniak, K., Gouvea, M.L., Hamdi, R., Hendry, M., Kanda, M., Kawai, T., Kawamoto, Y., Kondo, H., et al., 2011. Initial results from Phase 2 of the international urban energy balance model comparison. Int. J. Climatol. 272, 244–272. https://doi.org/10.1002/joc.2227.

Harshan, S., Roth, M., Velasco, E., Demuzere, M., 2017. Evaluation of an urban land surface scheme over a tropical suburban neighborhood. Theor. Appl. Climatol. 1–20. https://doi.org/10.1007/s00704-017-2221-7.

Ivanov, V.Y., Bras, R.L., Vivoni, E.R., 2008. Vegetation-hydrology dynamics in complex terrain of semiarid areas: 1. A mechanistic approach to modeling dynamic feedbacks. Water Resour. Res. 44 (October 2007) https://doi.org/10.1029/2006WR005588.

Jiao, M., Zhou, W., Zheng, Z., Wang, J., Qian, Y., 2017. Patch size of trees affects its cooling effectiveness: a perspective from shading and transpiration processes. Agric. For. Meteorol. 247 (May), 293–299. https://doi.org/10.1016/j.agrformet.2017.08.013.

Kent, C.W., Grimmond, S., Gatey, D., 2017. Aerodynamic roughness parameters in cities: inclusion of vegetation. J. Wind. Eng. Ind. Aerodyn. 169 (December 2016), 168–176. https://doi.org/10.1016/j.jweia.2017.07.016.

Klein, T., 2014. The variability of stomatal sensitivity to leaf water potential across tree species indicates a continuum between isohydric and anisohydric behaviours. Funct. Ecol. 28 (6), 1313–1320. https://doi.org/10.1111/1365-2435.12289.

Konarska, J., Uddling, J., Holmer, B., Lutz, M., Lindberg, F., Pleijel, H., Thorsson, S., 2015. Transpiration of urban trees and its cooling effect in a high latitude city. Int. J. Biometeorol. 60 (1), 159–172. https://doi.org/10.1007/s00484-015-1014-x.

Konarska, J., Holmer, B., Lindberg, F., Thorsson, S., 2016. Influence of vegetation and building geometry on the spatial variations of air temperature and cooling rates in a high-latitude city. Int. J. Climatol. 36 (5), 2379–2395. https://doi.org/10.1002/joc.4502.

Krayenhoff, E.S., Jiang, T., Christen, A., Martilli, A., Oke, T.R., Bailey, B.N., Nazarian, N., Voogt, J.A., Giometto, M.G., Stastny, A., Crawford, B.R., 2020. A multi-layer urban canopy meteorological model with trees (BEP-Tree): street tree impacts on pedestrian-level climate. Urban Clim. 32 (December 2019), 100590. https://doi.org/10.1016/j.uclim.2020.100590.

Macdonald, R.W., Griffiths, R.F., Hall, D.J., 1998. An improved method for the estimation of surface roughness of obstacle arrays. Atmos. Environ. 32 (11), 1857–1864.

Manickathan, L., Defraeye, T., Allegrini, J., Derome, D., Carmeliet, J., 2018. Parametric study of the influence of environmental factors and tree properties on the transpirative cooling effect of trees. Agric. For. Meteorol. 248 (October 2017), 259–274. https://doi.org/10.1016/j.agrformet.2017.10.014.

Manoli, G., Ivanov, V.Y., Fatichi, S., 2018. Dry-season greening and water stress in Amazonia: the role of modeling leaf phenology. J. Geophys. Res. Biogeosci. 123 (6), 1909–1926. https://doi.org/10.1029/2017JG004282.

Manoli, G., Fatichi, S., Schläpfer, M., Yu, K., Crowther, T.W., Meili, N., Burlando, P., Katul, G.G., Bou-Zeid, E., 2019. Magnitude of urban heat islands largely explained by climate and population. Nature 573 (7772), 55–60. https://doi.org/10.1038/s41586-019-1512-9.

Marchionni, V., Daly, E., Manoli, G., Tapper, N.J., Walker, J.P., Fatichi, S., 2020. Groundwater buffers drought effects and climate variability in urban reserves. Water Resour. Res. 56 (5), 1–19. https://doi.org/10.1029/2019WR026192.

Masson, V., 2000. A physically-based scheme for the urban energy budget in atmospheric models. Bound.-Layer Meteorol. 94 (September 1999), 357–397.

Mastrotheodoros, T., Pappas, C., Molnar, P., Burlando, P., Keenan, T.F., Gentine, P., Gough, C.M., Fatichi, S., 2017. Linking plant functional trait plasticity and the large increase in forest water use efficiency. J. Geophys. Res. Biogeosci. 122 (9), 2393–2408. https://doi.org/10.1002/2017JG003890.

McAdam, S.A.M., Brodribb, T.J., 2015. The evolution of mechanisms driving the stomatal response to vapor pressure deficit. Plant Physiol. 167 (3), 833–843. https://doi.org/10.1104/pp.114.252940.

Meili, N., Manoli, G., Burlando, P., Bou-Zeid, E., Chow, W.T., Coutts, A., Daly, E., Nice, K., Roth, M., Tapper, N., Velasco, E., Vivoni, E., Fatichi, S., 2020a. An urban ecohydrological model to quantify the effect of vegetation on urban climate and hydrology (UT&C v1.0). Geosci. Model. Dev. 13, 335–362. https://doi.org/10.5194/gmd-2019-225.

Meili, N., Manoli, G., Burlando, P., Bou-Zeid, E., Chow, W.T., Coutts, A., Daly, E., Nice, K., Roth, M., Tapper, N., Velasco, E., Vivoni, E., Fatichi, S., 2020b. Supplement of an urban ecohydrological model to quantify the effect of vegetation on urban climate and hydrology (UT & C v1. 0). Geosci. Model. Dev. 13, 335–362.

Meinzer, F.C., Woodruff, D.R., Marias, D.E., Smith, D.D., McCulloh, K.A., Howard, A.R., Magedman, A.L., 2016. Mapping 'hydroscapes' along the iso- to anisohydric continuum of stomatal regulation of plant water status. Ecol. Lett. 19 (11), 1343–1352. https://doi.org/10.1111/ele.12670.

Meteo Swiss, 2020. Meteorological Station Fluntern. In: https://www.meteoswiss.admin.ch/product/output/climate-data/climate-diagrams-normal-values-station-processing/SMA/climsheet_SMA_np8110_e.pdf.

Mexia, T., Vieira, J., Príncipe, A., Anjos, A., Silva, P., Lopes, N., Freitas, C., Santos-Reis, M., Correia, O., Branquinho, C., Pinho, P., 2018. Ecosystem services: urban parks under a magnifying glass. Environ. Res. 160 (August 2017), 469–478. https://doi.org/10.1016/j.envres.2017.10.023.

Middel, A., Chhetri, N., Quay, R., 2015. Urban forestry and cool roofs: Assessment of heat mitigation strategies in Phoenix residential neighborhoods. Urban For. Urban Green. 14 (1), 178–186. https://doi.org/10.1016/j.ufug.2014.09.010.

Middel, A., Selover, N., Hagen, B., Chhetri, N., 2016. Impact of shade on outdoor thermal comfort—a seasonal field study in Tempe, Arizona. Int. J. Biometeorol. 60 (12), 1849–1861. https://doi.org/10.1007/s00484-016-1172-5.

Monteith, J.L., 1995. A reinterpretation of stomatal responses to humidity. Plant Cell Environ. 18 (4), 357–364. https://doi.org/10.1111/j.1365-3040.1995.tb00371.x.

Moonen, P., Gromke, C., Dorer, V., 2013. Performance assessment of Large Eddy Simulation (LES) for modeling dispersion in an urban street canyon with tree planting. Atmos. Environ. 75, 66–76. https://doi.org/10.1016/j.atmosenv.2013.04.016.

Morakinyo, T.E., Lam, Y.F., 2016. Simulation study on the impact of tree-configuration, planting pattern and wind condition on street-canyon's micro-climate and thermal comfort. Build. Environ. 103, 262–275. https://doi.org/10.1016/j.buildenv.2016.04.025.

Morakinyo, T.E., Kong, L., Lau, K.K.L., Yuan, C., Ng, E., 2017. A study on the impact of shadow-cast and tree species on in-canyon and neighborhood's thermal comfort. Build. Environ. 115, 1–17. https://doi.org/10.1016/j.buildenv.2017.01.005.

Morison, J.I.L., Gifford, R.M., 1983. Stomatal sensitivity to Carbon Dioxide and humidity: a comparison of two C3 and two C4 grass species. Plant Physiol. 71 (4), 789–796. https://doi.org/10.1104/pp.71.4.789.

Mussetti, G., Brunner, D., Allegrini, J., Wicki, A., Schubert, S., Carmeliet, J., 2019. Simulating urban climate at sub-kilometre scale for representing the intra-urban variability of Zurich, Switzerland. Int. J. Climatol. 40 (1), 458–476. https://doi.org/10.1002/joc.6221.

Mussetti, G., Brunner, D., Henne, S., Allegrini, J., Krayenhoff, E.S., Schubert, S., Feigenwinter, C., Vogt, R., Wicki, A., Carmeliet, J., 2020. COSMO-BEP-Tree v1.0: a coupled urban climate model with explicit representation of street trees. Geosci. Model. Dev. 13 (3), 1685–1710. https://doi.org/10.5194/gmd-13-1685-2020.

Ng, K.S.T., Sia, A., Ng, M.K.W., Tan, C.T.Y., Chan, H.Y., Tan, C.H., Rawtaer, I., Feng, L., Mahendran, R., Larbi, A., Kua, E.H., Ho, R.C.M., 2018. Effects of horticultural therapy on asian older adults: a randomized controlled trial. Int. J. Environ. Res. Public Health 15 (8), 1–14. https://doi.org/10.3390/ijerph15081705.

Nice, K.A., Coutts, A.M., Tapper, N.J., 2018. Development of the VTUF-3D v1.0 urban micro-climate model to support assessment of urban vegetation influences on human thermal comfort. Urban Clim. 1–25. https://doi.org/10.1016/j.uclim.2017.12.008.

Oren, R., Sperry, J.S., Katul, G.G., Pataki, D.E., Ewers, B.E., Phillips, N., Schäfer, K.V.R., 1999. Survey and synthesis of intra- and interspecific variation in stomatal sensitivity to vapour pressure deficit. Plant Cell Environ. 22 (12), 1515–1526. https://doi.org/10.1046/j.1365-3040.1999.00513.x.

Ossola, A., Hahs, A.K., Nash, M.A., Livesley, S.J., 2016. Habitat complexity enhances comminution and decomposition processes in urban ecosystems. Ecosystems 19 (5), 927–941. https://doi.org/10.1007/s10021-016-9976-z.

Ow, L.F., Ghosh, S., Yusof, M.L.M., 2019. Growth of Samanea saman: estimated cooling potential of this tree in an urban environment. Urban For. Urban Green. 41 (March), 264–271. https://doi.org/10.1016/j.ufug.2019.03.021.

Paschalis, A., Fatichi, S., Katul, G.G., Ivanov, V.Y., 2015. Cross-scale impact of climate temporal variability on ecosystem water and carbon fluxes. J. Geophys. Res. G: Biogeosci. 120 (9), 1716–1740. https://doi.org/10.1002/2015JG003002.

Pataki, D.E., Carreiro, M.M., Cherrier, J., Grulke, N.E., Jennings, V., Pincetl, S., Pouyat, R.V., Whitlow, T.H., Zipperer, W.C., 2011. Coupling biogeochemical cycles in urban environments: ecosystem services, green solutions, and misconceptions. Front. Ecol. Environ. 9 (1), 27–36. https://doi.org/10.1890/090220.

Rahman, M.A., Smith, J.G., Stringer, P., Ennos, A.R., 2011. Effect of rooting conditions on the growth and cooling ability of Pyrus calleryana. Urban For. Urban Green. 10 (3), 185–192. https://doi.org/10.1016/j.ufug.2011.05.003.

Rahman, Mohammad A., Moser, A., Rötzer, T., Pauleit, S., 2017. Within canopy temperature differences and cooling ability of Tilia cordata trees grown in urban conditions. Build. Environ. 114, 118–128. https://doi.org/10.1016/j.buildenv.2016.12.013.

Rahman, Mohammad A., Moser, A., Gold, A., Rötzer, T., Pauleit, S., 2018. Vertical air temperature gradients under the shade of two contrasting urban tree species during different types of summer days. Sci. Total Environ. 633, 100–111. https://doi.org/10.1016/j.scitotenv.2018.03.168.

Rahman, Mohammad A., Moser, A., Rötzer, T., Pauleit, S., 2019. Comparing the transpirational and shading effects of two contrasting urban tree species. Urban Ecosyst. 22 (4), 683–697. https://doi.org/10.1007/s11252-019-00853-x.

Redon, E., Lemonsu, A., Masson, V., 2020. An urban trees parameterization for modeling microclimatic variables and thermal comfort conditions at street level with the Town Energy Balance model (TEB-SURFEX v8.0). Geosci. Model. Dev. 13 (2), 385–399. https://doi.org/10.5194/gmd-13-385-2020.

Richards, D.R., Fung, T.K., Belcher, R.N., Edwards, P.J., 2020. Differential air temperature cooling performance of urban vegetation types in the tropics. Urban For. Urban Green. 50 (June 2019) https://doi.org/10.1016/j.ufug.2020.126651.

Rockel, B., Will, A., Hense, A., 2008. The regional climate model COSMO-CLM (CCLM). Meteorol. Z. 17 (4), 347–348. https://doi.org/10.1127/0941-2948/2008/0309.

Roman, D.T., Novick, K.A., Brzostek, E.R., Dragoni, D., Rahman, F., Phillips, R.P., 2015. The role of isohydric and anisohydric species in determining ecosystem-scale response to severe drought. Oecologia 179 (3), 641–654. https://doi.org/10.1007/s00442-015-3380-9.

Roth, M., Jansson, C., Velasco, E., 2017. Multi-year energy balance and carbon dioxide fluxes over a residential neighbourhood in a tropical city. Int. J. Climatol. 37 (5), 2679–2698. https://doi.org/10.1002/joc.4873.

Rutter, A.J., Kershaw, K.A., Robins, P.C., Morton, A.J., 1971. A predictive model of rainfall interception in forests, 1. Derviation of the model from observations in a plantation of corsican pine. Agric. Meteorol. 9 (1969), 367–384.

Rutter, A.J., Morton, A.J., Robins, P.C., 1975. A predictive model of rainfall interception in forests. 2. Generalization of model and comparison with observations in some coniferous and hardwood stands. J. Appl. Ecol. 12, 367–380.

Salmond, J.A., Tadaki, M., Vardoulakis, S., Arbuthnott, K., Coutts, A., Demuzere, M., Dirks, K.N., Heaviside, C., Lim, S., Macintyre, H., Mcinnes, R.N., Wheeler, B.W., 2016. Health and climate related ecosystem services provided by street trees in the urban environment. Environ. Health 15 (Suppl 1). https://doi.org/10.1186/s12940-016-0103-6.

Saneinejad, S., Moonen, P., Carmeliet, J., 2014. Coupled CFD, radiation and porous media model for evaluating the micro-climate in an urban environment. J. Wind. Eng. Ind. Aerodyn. 128, 1–11. https://doi.org/10.1016/j.jweia.2014.02.005.

Shashua-Bar, L., Pearlmutter, D., Erell, E., 2009. The cooling efficiency of urban landscape strategies in a hot dry climate. Landsc. Urban Plan. 92 (3–4), 179–186. https://doi.org/10.1016/j.landurbplan.2009.04.005.

Shashua-Bar, L., Pearlmutter, D., Erell, E., 2011. The influence of trees and grass on outdoor thermal comfort in a hot-arid environment. Int. J. Climatol. 31 (10), 1498–1506. https://doi.org/10.1002/joc.2177.

Skamarock, W.C., Klemp, J.B., Dudhia, J., Gill, D.O., Barker, D.M., Duda, M.G., Huang, X.-Y., Wang, W., Powers, J.G., 2008. A Description of the Advanced Research WRF Version 3. NCAR Technical Note. https://doi.org/10.1080/07377366.2001.10400427.

Song, J., Wang, Z.H., 2015. Interfacing the urban land–Atmosphere system through coupled urban canopy and atmospheric models. Bound.-Layer Meteorol. 154 (3), 427–448. https://doi.org/10.1007/s10546-014-9980-9.

Spangenberg, J., Shinzato, P., Johansson, E., Duarte, D., 2008. Simulation of the influence of vegetation on microclimate and thermal comfort in the city of São Paulo. Revista Da Sociedade Brasileira de Arborização Urbana 3 (2), 1–19. https://doi.org/10.5380/revsbau.v3i2.66265.

Stewart, I.D., Oke, T.R., 2012. Local climate zones for urban temperature studies. Am. Meteorol. Soc. https://doi.org/10.1175/BAMS-D-11-00019.1.

Stratópoulos, L.M.F., Duthweiler, S., Häberle, K.H., Pauleit, S., 2018. Effect of native habitat on the cooling ability of six nursery-grown tree species and cultivars for future roadside plantings. Urban For. Urban Green. 30 (January), 37–45. https://doi.org/10.1016/j.ufug.2018.01.011.

Sturman, A.P., Tapper, N.J., 2006. The Weather and Climate of Australia and New Zealand, 2nd ed. Oxford University Press.

Tan, C.L., Wong, N.H., Jusuf, S.K., 2014. Effects of vertical greenery on mean radiant temperature in the tropical urban environment. Landsc. Urban Plan. 127, 52–64. https://doi.org/10.1016/j.landurbplan.2014.04.005.

Tan, P.Y., Wong, N.H., Tan, C.L., Jusuf, S.K., Chang, M.F., Chiam, Z.Q., 2018. A method to partition the relative effects of evaporative cooling and shading on air temperature within vegetation canopy. J. Urban Ecol. 4 (1), 1–11. https://doi.org/10.1093/jue/juy012.

Upreti, R., Wang, Z.H., Yang, J., 2017. Radiative shading effect of urban trees on cooling the regional built environment. Urban For. Urban Green. 26 (May), 18–24. https://doi.org/10.1016/j.ufug.2017.05.008.

Velasco, E., Roth, M., Tan, S.H., Quak, M., Nabarro, S.D.A., Norford, L., 2013. The role of vegetation in the CO2 flux from a tropical urban neighbourhood. Atmos. Chem. Phys. 13, 10185–10202. https://doi.org/10.5194/acp-13-10185-2013.

Wang, Z., Bou-zeid, E., Smith, J.A., 2013. A coupled energy transport and hydrological model for urban canopies evaluated using a wireless sensor network. Q. J. R. Meteorol. Soc. 139 (July), 1643–1657. https://doi.org/10.1002/qj.2032.

Wang, Z.H., Zhao, X., Yang, J., Song, J., 2016. Cooling and energy saving potentials of shade trees and urban lawns in a desert city. Appl. Energy 161, 437–444. https://doi.org/10.1016/j.apenergy.2015.10.047.

Wang, C., Wang, Z.H., Yang, J., 2018. Cooling effect of urban trees on the built environment of contiguous united states. Earths Future 6 (8), 1066–1081. https://doi.org/10.1029/2018EF000891.

Wang, C., Wang, Z.H., Wang, C., Myint, S.W., 2019. Environmental cooling provided by urban trees under extreme heat and cold waves in U.S. Cities. Remote Sens. Environ. 227 (January), 28–43. https://doi.org/10.1016/j.rse.2019.03.024.

Willis, K.J., Petrokofsky, G., 2017. The natural capital of city trees. Science 356 (6336), 374–376. https://doi.org/10.1126/science.aam9724.

Yang, J., Bou-Zeid, E., 2018. Should cities embrace their heat islands as shields from extreme cold? J. Appl. Meteorol. Climatol. 57 (6), 1309–1320. https://doi.org/10.1175/JAMC-D-17-0265.1.

Yang, J., Wang, Z.H., Chen, F., Miao, S., Tewari, M., Voogt, J.A., Myint, S., 2015. Enhancing hydrologic modelling in the coupled weather research and forecasting–Urban modelling system. Bound.-Layer Meteorol. 155 (1), 87–109. https://doi.org/10.1007/s10546-014-9991-6.

Ziter, C.D., Pedersen, E.J., Kucharik, C.J., Turner, M.G., 2019. Scale-dependent interactions between tree canopy cover and impervious surfaces reduce daytime urban heat during summer. Proc. Natl. Acad. Sci. U.S.A. 116 (15), 7575–7580. https://doi.org/10.1073/pnas.1817561116.

Zölch, T., Rahman, M.A., Pfleiderer, E., Wagner, G., Pauleit, S., 2019. Designing public squares with green infrastructure to optimize human thermal comfort. Build. Environ. 149 (October 2018), 640–654. https://doi.org/10.1016/j.buildenv.2018.12.051.